

10 CFR 50.55a

November 25, 2003
5928-03-20236

U. S. Nuclear Regulatory Commission
Attn: Document Control Desk
Washington, DC 20555

Three Mile Island, Unit 1
Operating License No. DPR-50
NRC Docket No. 50-289

Subject: Additional Information Concerning a Proposed Alternative Associated with the Use of a Weld Overlay

- References:
- 1) Letter from Michael P. Gallagher (AmerGen Energy Company, LLC), to U. S. Nuclear Regulatory Commission, dated November 3, 2003
 - 2) Letter from Michael P. Gallagher (AmerGen Energy Company, LLC), to U. S. Nuclear Regulatory Commission, dated November 7, 2003
 - 3) Letter from Michael P. Gallagher (AmerGen Energy Company, LLC), to U. S. Nuclear Regulatory Commission, dated November 18, 2003
 - 4) Letter from Michael P. Gallagher (AmerGen Energy Company, LLC), to U. S. Nuclear Regulatory Commission, dated November 20, 2003

Dear Sir or Madam:

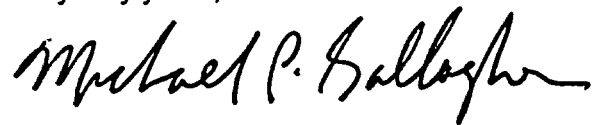
In the Referenced letters, AmerGen Energy Company (AmerGen) requested a proposed alternative in accordance with 10 CFR 50.55a, "Codes and standards," paragraph (a)(3)(i) and supplied additional information requested by the U. S. Nuclear Regulatory Commission. This proposed alternative would permit the use of a full structural weld overlay repair for an indication identified in the steam generator "A" hot leg surge line nozzle-to-safe end weld. In the Reference 4 letter, AmerGen provided a proprietary version of the summary of the weld overlay design and analysis. Attachment 1 to this letter provides a non-proprietary version of that document.

A047

Additional Information Concerning a Proposed
Alternative Associated with the Use of a Weld Overlay
November 25, 2003
Page 2

If you have any questions, please contact us.

Very truly yours,

A handwritten signature in black ink that reads "Michael P. Gallagher". The signature is written in a cursive style with a long, sweeping underline.

Michael P. Gallagher
Director, Licensing and Regulatory Affairs
AmerGen Energy Company, LLC

Attachment

cc: H. J. Miller, Administrator, Region I, USNRC
D. M. Kern, USNRC Senior Resident Inspector, TMI
D. M. Skay, USNRC Senior Project Manager
File No. 01086

ATTACHMENT 1

**NON-PROPRIETARY VERSION
SUMMARY OF WELD OVERLAY DESIGN AND ANALYSIS**

Report No.: SIR-03-155
Revision No.: 0
Project No.: TMI-03Q
File No.: TMI-03Q-402
November 2003
Non-Proprietary Version of
SIR-03-153, Rev. 0

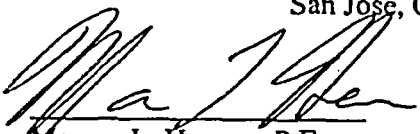
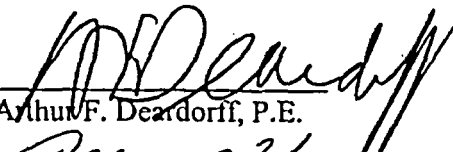
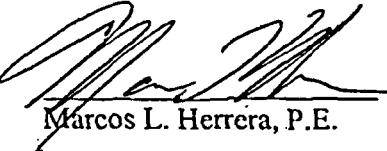
Note: Information considered to be "Framatome Proprietary"
have been removed and denoted by "[REDACTED]"

**Weld Overlay Design for the
Hot Leg Nozzle to Surge Line Weld at
Three Mile Island Unit 1**

Prepared for:
AmerGen Energy Company, LLC

Prepared by:

Structural Integrity Associates, Inc.
San Jose, California

<i>Prepared by:</i>		Date: <u>11/25/03</u>
	Marcos L. Herrera, P.E.	
<i>Reviewed by:</i>		Date: <u>11/25/03</u>
	Shu S. Tang, P.E.	
<i>Reviewed by:</i>		Date: <u>11/25/03</u>
	Arthur F. Deardorff, P.E.	
<i>Approved by:</i>		Date: <u>11/25/03</u>
	Marcos L. Herrera, P.E.	

REVISION CONTROL SHEET

Document Number: SIR-03-155

Title: Weld Overlay Design for the Surge Line to Hot Leg Nozzle at Three Mile Island Unit 1

Client: AmerGen Energy Company, LLC

SI Project Number: TMI-03Q

Section	Pages	Revision	Date	Comments
1	1-1 - 1-3	0	11/21/03	Initial Issue
2	2-1 - 2-11			
3	3-1 - 3-7			
4	4-1 - 4-17			
5	5-1 - 5-3			
6	6-1 - 6-2			
7	7-1			

Table of Contents

<u>Section</u>	<u>Page</u>
1.0 INTRODUCTION	1-1
2.0 WELD OVERLAY DESIGN	2-1
2.1 Design Criteria.....	2-1
2.2 Weld Overlay Thickness and Length.....	2-2
2.2.1 <i>Use of Equations in Appendix C, Section XI of the ASME Code</i>	2-3
2.2.2 <i>Use of 75% Maximum Allowable Flaw Criteria</i>	2-7
2.3 Weld Overlay Design For PWSCC.....	2-8
3.0 WELD RESIDUAL STRESS ANALYSIS	3-1
3.1 Weld Parameters	3-2
3.1.1 <i>Original ID Weld Repair Weld Parameters</i>	3-2
3.1.2 <i>Weld Overlay Weld Parameters</i>	3-2
3.2 Finite Element Model	3-3
3.3 Residual Stress Results	3-4
4.0 CRACK GROWTH EVALUATION	4-1
4.1 PWSCC.....	4-2
4.1.1 <i>Axial Flaw Crack Growth</i>	4-2
4.1.2 <i>Circumferential Flaw Growth</i>	4-3
4.1.3 <i>Alloy 52 PWSCC</i>	4-3
4.1.4 <i>PWSCC Conclusion</i>	4-4
4.2 Fatigue Crack Growth.....	4-5
4.2.1 <i>Fatigue Crack Growth Technical Approach and Methodology</i>	4-5
4.2.2 <i>Crack Growth Rate</i>	4-9
4.3 Fatigue Crack Growth Analysis Procedure.....	4-10
4.4 Results of Fatigue Crack Growth Analysis.....	4-11
4.5 Final Weld Overlay Design	4-12
5.0 STRESS REPORT RECONCILIATION.....	5-1
6.0 CONCLUSIONS.....	6-1
7.0 REFERENCES	7-1

List of Figures

<u>Figure</u>	<u>Page</u>
Figure 1-1. Three Mile Island Unit 1 Power Plant, Hot Leg Nozzle-to-Surge Line Weld	Error! Bookmark not defined.
Figure 2-1. Weld Overlay Design	2-10
Figure 2-2. Weld Overlay Design (Cont'd).....	2-11
Figure 3-1. Schematic of ID Weld Repair	3-5
Figure 3-2. Finite Element Model For Weld Residual Stress Analysis	3-6
Figure 3-3. Residual Stress Distribution in Vicinity of Weld Due to Weld Repair and Weld Overlay.....	3-7
Figure 4-1. Final Crack Size for Axial Crack in Weld - Postulated Circumferential Crack in Weld.....	4-14
Figure 4-2. Final Crack Size for Postulated Circumferential Crack in Weld	4-15
Figure 4-3. Contribution of Various Transients to Crack Growth Postulated Circumferential Crack for Alloy 600 Crack Growth Rate	4-16
Figure 4-4. Crack Growth for Postulated Circumferential Crack – Alloy 600 Crack Growth Law	4-17

List of Tables

<u>Table</u>	<u>Page</u>
Table 4-4. Crack Growth Results.....	4-13

1.0 INTRODUCTION

This report presents the weld overlay design and analysis for AmerGen's Three Mile Island (TMI) Unit 1 Hot Leg Nozzle-to-Surge Line weld (Weld No. SR0010BM). During the 1R15 ISI examinations, an axial flaw 0.51" deep (including uncertainty) was detected in the weld near the [REDACTED] pipe-to-safe end interface. It is likely that the degradation mechanism is primary water stress corrosion cracking (PWSCC). It should be noted that this location is also subjected to significant thermal stress cycling including stratification and striping. However, the characteristics of the flaw do not appear to be consistent with those for fatigue cracking.

This weld connects an [REDACTED] nozzle, to an [REDACTED] safe end (similar to [REDACTED]). The safe end and connected surge line piping are nominally [REDACTED]. The original butt weld was constructed from [REDACTED]. The indication appears to be located in the [REDACTED] weld material. The function of the nozzle is to connect the pressurizer surge line to the Once Through Steam Generator (OTSG) "A" [REDACTED] hot leg. Figure 1-1 shows the nozzle geometry and general location of the indication.

AmerGen has prepared a customized temper bead weld overlay repair to disposition the flawed weldment. The weld filler material will be Alloy 52. Weld overlays have been used extensively in the Boiling Water Reactor (BWR) nuclear industry to repair flawed weldments since 1982. In addition, a significant amount of weld butter was applied to the V.C. Summer Reactor Coolant System (RCS) nozzle in 2002. On many occasions, weld overlays have been applied to Pressurized Water Reactor (PWR) Control Rod Drive Mechanism (CRDM) canopy seal welds (CSW).

Weld overlays involve the application of weld metal circumferentially around the pipe in the vicinity of the flawed weldment to restore ASME Code Section XI margins [1] as allowed by ASME Code Case N-504-2 [2]. The application of weld overlay repairs at BWRs has also been shown to produce favorable compressive residual stresses on the inner portion of the pipe wall, which minimizes further crack growth. Many BWR weld overlays were applied using stainless

steel and in recent years, Alloy 52 has been used. In this case, the overlay is welded using Alloy 52 filler material, which has excellent resistance to stress corrosion cracking (SCC).

Thus, the TMI Unit 1 weld overlay design is performed using the standard approach in the design of hundreds of overlays applied to BWR piping and nozzles to address intergranular stress corrosion cracking (IGSCC). Additional analyses were performed to verify that fatigue crack growth does not impact the overlay design since the location is subjected to significant temperature and nozzle loading variations due to stratification and thermal transients.

In applying a weld overlay to the nozzle-to-safe end location using Code Case N-504-2, several issues need to be addressed to assure the appropriateness and effectiveness of the repair.

Following are the aspects that must be considered:

1. **Stress Limits at Overlay Location:** The overlay thickness and length must meet ASME Code Case N-504-2 [2] and NUREG-0313, Rev. 2 [3] requirements. This aspect includes consideration for PWSCC and fatigue crack growth.
2. **Inspection capability:** The weld overlay geometry must allow for performance of required inspections.
3. **Impact on Connected Piping System:** The piping system requirements must still be satisfied when axial and circumferential shrinkage caused by the overlay application is considered.
4. **Nozzle/Safe End Stress and Fatigue Reconciliation:** The existing Stress Report for the surge line piping must be reconciled by including the effect of the overlay on thermal stresses and fatigue due to transients. This includes both stress and fatigue impact on the nozzle/safe end region.

This report provides the details to the items listed above as well as providing the actual design of the overlay. It also incorporates the inspection capability requirements as provided by AmerGen.

The actual measured axial shrinkage will be used to assess the impact of the overlay on the connected piping although a conservative value has been used in the analysis and has been shown to have a negligible effect on the relatively flexible surge line piping. The assumed axial shrinkage used in the current evaluation is considered conservative and bounding. AmerGen will measure the actual axial shrinkage to justify the applicability of the piping analysis results.

Figure 1-1. Three Mile Island Power Plant Unit 1 Hot Leg Nozzle-to-Surge Line Weld

2.0 WELD OVERLAY DESIGN

The overlay design presented in this section is performed with the initial assumption that PWSCC is the crack growth mechanism. It will be further assumed that the flaw is through the original pipe wall from the aspect of the structural design. The assumption of a through-original-wall flaw is acceptable for the design of the overlay but highly conservative with respect to the actual flaw condition since only a part-through-wall axial flaw was found. Even if the flaw were to grow through the safe end to the overlay, PWSCC growth into the overlay material is not expected due to the resistance to PWSCC. Due to the thermal cycling experienced at this location, fatigue crack growth was also evaluated as is presented in Section 3.0, both for the observed flaw and for the postulated circumferential flaw. Results of the crack growth analysis will confirm the acceptability of the weld overlay design considering both PWSCC and fatigue loading.

2.1 Design Criteria

The weld overlay was designed as a full structural overlay in accordance with the requirements of NUREG-0313, Revision 2 [3] (which was implemented by Generic Letter 88-01 [13], ASME Code Case N-504 [2], Section XI of the ASME Boiler and Pressure Vessel Code, Paragraph IWB-3640 [1]). The overlay will extend around the full circumference of the nozzle-to-pipe junction for the required length. It was designed by assuming the weld to contain a fully circumferential through-original-wall flaw. The flaw was also assumed to extend through the initial layers of the overlay intended for dilution considerations. In effect, credit was not taken for the first two layers conservatively assuming that these layers remain susceptible to PWSCC due to possible dilution of the Alloy 52 weld overlay material from the underlying weld and base material. Thus, the first two layers are considered part of the original wall for this sizing calculation. The thickness of the overlay was determined by comparing the stress in the pipe with the weld overlay for a combination of dead weight, internal pressure and seismic stresses with the criteria contained in Paragraph IWB-3641 [1]. Both normal/upset and emergency/faulted conditions were considered in the evaluation.

Per Code Case N-504-2, the overlay design must also meet the ASME Code, Section III stress limits for primary local and bending stress and secondary peak stress.

Specifically, Tables IWB 3641-1 and IWB 3641-2 or the equations in Appendix C of ASME Code Section XI can be used to initially size the overlay. These tables and the appropriate equation will be used for the gas tungsten arc welding (GTAW) process, which will be used to apply the overlay. The overlay material will be PWSCC-resistant Alloy 52. The results of this calculation must be compared against the other requirements (fatigue crack growth, UT sizing, etc.) to finalize the weld overlay thickness.

2.2 Weld Overlay Thickness and Length

This section contains the discussion on the determination of the weld overlay thickness and length. Three approaches were considered in the determination of the weld overlay thickness. These three approaches are:

- Use of the source equations in Appendix C, Section XI of the ASME Code.
- Use of 75% maximum allowable flaw criteria (per IWB-3640 of ASME Code Section XI).
- Use of ASME Code Section III stress limits (per Code Case N-504-2).

The bounding thickness (maximum) of these three approaches will be taken as the minimum required overlay thickness. Each of these approaches is summarized below. The third item above, per Code Case N-504-2, is satisfied if the recommended lengths are met. Since in this case the resulting overlay length is well in excess of the recommended Code Case N-504-2 length (see Section 2.2.1.3), this criterion is satisfied and the first two criteria are used to define the overlay thickness.

2.2.1 Use of Equations in Appendix C, Section XI of the ASME Code

The weld overlay thickness, per ASME Code Case N-504-2, is designed using the equations provided in Appendix C of the ASME Code, Section XI. These equations are based on net-section plastic collapse. At the point of collapse, the equations, which describe the equilibrium condition, are (from Reference 1 for $\alpha + \beta > \pi$):

$$\beta = [(1-d/t - P_m/\sigma_f)\pi]/(2-d/t) \quad (2-1)$$

$$P_b' = (2\sigma_f/\pi)[(2-d/t)\sin(\beta)] \quad (2-2)$$

where:

- β = angle of neutral axis
- P_m = primary membrane stress
- σ_f = flow stress of material = $3S_m$
- S_m = design stress intensity
- d = crack depth
- t = thickness
- P_b = primary bending stress
- P_b' = primary bending stress at collapse

P_m and P_b are determined from the applied primary loads at the location of the crack for the original uncracked condition and are modified to account for the additional weld overlay thickness (in the iterative solution of Equations 2-1 and 2-2). The condition based on equilibrium, which must be satisfied, is:

$$P_m + P_b' = SF (P_m + P_b) \quad (2-3)$$

where SF = safety factor =

- 2.77 for normal or upset (N/U) condition
- 1.39 for emergency or faulted (E/F) condition

2.2.1.1 Stress Calculation

The stresses must consider the limiting stress conditions and include required safety factors (normal, upset, emergency and faulted). The determination of the weld overlay thickness is performed using the limit load (net-section collapse) analysis described above. Since the overlay will be applied using a non-flux weld process (GTAW), only the primary stresses need to be considered. The primary stresses are those due to pressure, seismic and dead weight loads. Stresses due to piping thermal expansion and transients need not be included.

The primary membrane and bending stresses in the un-overlayed safe end can be calculated as follows:

Primary membrane = P_m = membrane stress due to pressure, deadweight and seismic loads.

$$P_m = PR/2t + (F_{x,DW} + F_{x,seismic})/A$$

where P = internal pressure (1500 psi for upset condition [14])
 R = radius of original pipe (150 on nozzle side, 100 on safe end side)
 A = cross sectional area of original safe end or nozzle
 F_x = axial load
 t = thickness (1.5 on nozzle side, 1.0 on safe end side)

Primary bending = P_b = bending stress due to seismic loads.

$$P_b = (DW+SEISMIC)/Z$$

where DW = moment due to deadweight
 $SEISMIC$ = moment due to seismic and other loading
 Z = section modulus

The limiting load combinations were:

Normal/Upset (N/U): P + OBE+ DW
Emergency/Faulted (E/F): P + SSE + DW

where: OBE = operating basis earthquake inertia loads
 SSE = safe shutdown earthquake inertia loads

The applicable forces and moments are shown in Table 2-1 [4].

Note that since the ratio of the safety factors between N/U and E/F conditions is 2, the N/U condition will govern in this case since the ratio of the faulted pressure to upset pressure is well below 2. The SSE loads are twice that for the OBE loads (See Table 2-1). Thus, only the upset condition will be evaluated further in this evaluation.

Substituting the geometry and loads, from Table 2-1, into Equations 2-1 and 2-2 results in a primary membrane stress of [REDACTED] ksi and [REDACTED] ksi for the safe end side and nozzle side respectively. The primary bending stress is [REDACTED] ksi and [REDACTED] ksi for the safe end and nozzle side, respectively. Note that shear loads do not contribute to any normal stress. The stresses listed above are for the as-welded pipe prior to application of the weld overlay.

2.2.1.2 Weld Overlay Thickness Calculation

The overlay thickness is dependent on the allowable material design stress intensity, S_m . The S_m for the Alloy 52 weld overlay material is taken as the limiting S_m for the underlying base materials. Although it could be justified to use the S_m for Alloy 600, this conservatism will be introduced in order to add additional margin. For this case, the overlay is being applied onto [REDACTED] weld, and [REDACTED] weld butter material. The limiting S_m is for the [REDACTED] material that has an S_m of [REDACTED] ksi at [REDACTED] [5]. Note that this compares against an S_m of 23.3 ksi for the Ni-Cr-Fe overlay material.

The pc-CRACK computer program [6], was used to determine the weld overlay thickness. The following cases were evaluated:

Nozzle Side of Weld

t	=	
S _m	=	
3S _m	=	
P _m	=	
P _b	=	
SF	=	

Safe End Side of Weld

t	=	
S _m	=	
3S _m	=	
P _m	=	
P _b	=	
SF	=	

Results of the pc-CRACK analysis give a required weld overlay thickness of approximately 0.437” and 0.444” on the pipe and nozzle side of the weld, respectively. The thickness would be even less if the S_m for Ni-Cr-Fe were to be used.

2.2.1.3 Weld Overlay Length

Code Case N-504-2 gives guidance on the weld overlay length. Ideally for a full structural overlay in order to assure that stress limits and transfer of the load from the pipe to the overlay and back to the pipe, the length of the overlay on each side from the location of the flaw is recommended to be:

$$l = 0.75\sqrt{(Rt)} \tag{2-4}$$

- where R = pipe outer radius
- t = pipe nominal wall thickness

Note that this length is not a requirement, but provided as a guide to determine the length that avoids end effects and provide a smooth transition of the load path from the original pipe to the overlay. Substitution of the nozzle geometry into Equation 2-4 results in a length of 1.84” and 2.08” on the safe end and nozzle side, respectively. This length should be measured from any possible location of the indication assuming it to grow through-wall. If it is assumed that the crack can grow anywhere through the susceptible Alloy 182 material, then a more appropriate measurement assuring the recommended length from any possible through-wall crack location would be measured from the outside diameter surface interface of the Alloy 182 material and

Solving for t_{wol} gives the weld overlay minimum thickness of 0.51" on the [REDACTED] side of the weld, which is the limiting side since it is thicker than the [REDACTED] side of the weld. This thickness is that part of the deposited Alloy 52 material that is assumed to withstand the applied loads. Since this overlay thickness is the minimum acceptable per ASME Code Section XI in order to meet the requirement that no flaw greater than 75% of wall is permitted, the overlay thickness must be at least 0.51", beyond the first two layers (dilution layers), which are not considered.

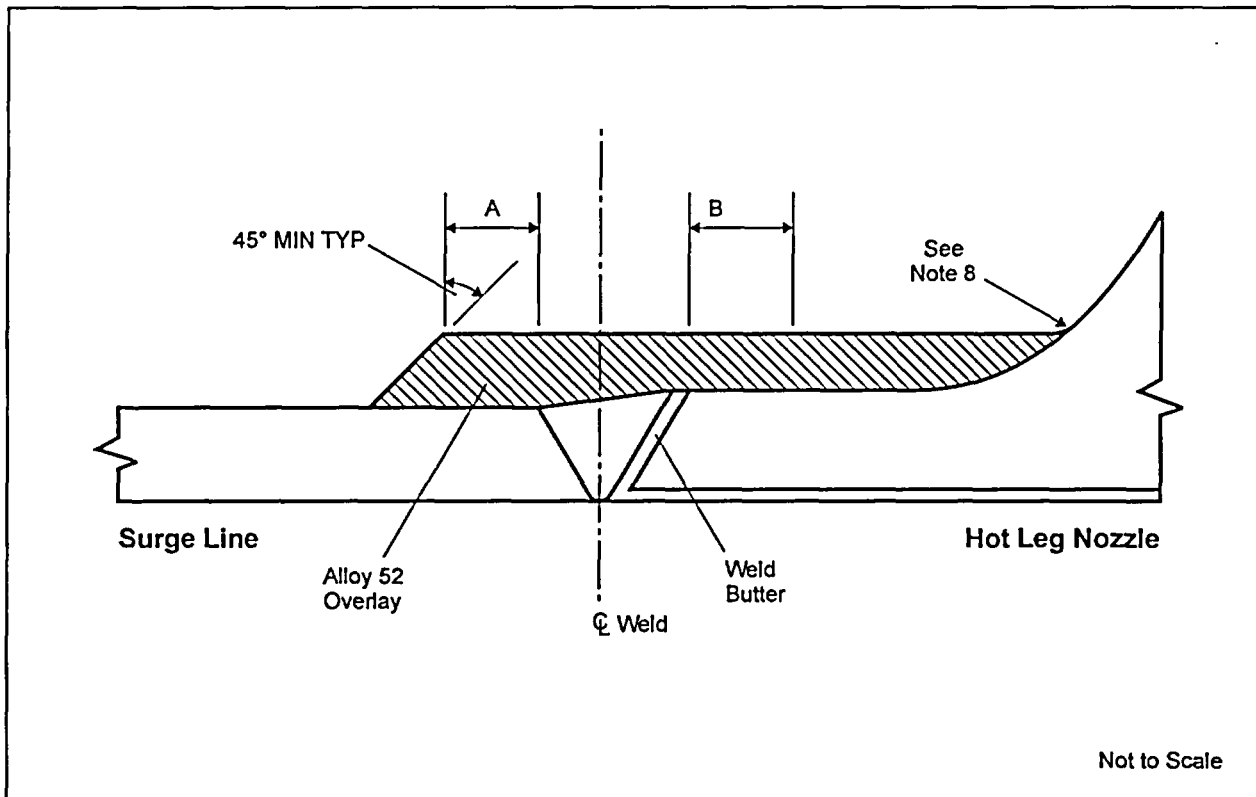
2.3 Weld Overlay Design For PWSCC

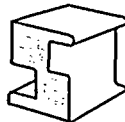
Based on the calculation discussion in this section and considering UT inspectability, the weld overlay design considering PWSCC only is shown in Figure 2-1 and 2-2. Note that the design has been modified to account for UT inspectability. The length of the overlay was extended to blend into the nozzle outside diameter taper. This allows for UT inspection and avoids a concentration on the nozzle OD. In addition, the length on the pipe side of the weld was extended to approximately 2.5". Although the diameter of the safe end is smaller than that of the nozzle, the thickness of the overlay on the safe end side was made such that the weld overlay outer radius was constant to create a flat surface for UT inspectability.

Table 2-1
Loads at Nozzle-to-Safe End Location



The table content is completely redacted with a large black rectangular box. The box is bounded by square brackets on the left and right sides, indicating it spans the width of the table.



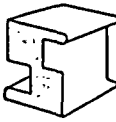
WELD	FLAW CHARACTERIZATION	DESIGN DIMENSIONS			COMMENTS
		t	A	B	
Hot Leg Nozzle to Surge Line Weld	Assumed 360° Circ. 100% Throughwall Flaw	0.51" see Note 4	1.9" (min)	2.1" (min)	Recommend Blend Into Nozzle
1	MLH 11/10/03	AJG 11/10/03	MLH 11/10/03		Editorial change only; no design change.
0	MLH 11/3/03	AJG 11/3/03	MLH 11/3/03		
Revision	Prepared by/ Date	Checked by/ Date	Approved by/ Date		COMMENTS
Job No:	TMI-03Q	Plant/Unit:	Three Mile Island Unit 1		
File No:	TMI-03Q-501	 STRUCTURAL INTEGRITY ASSOCIATES, INC.			
Drawing No:	TMI-03Q-01			Title: Standard Weld Overlay Design	Sheet <u>1</u> of <u>2</u>

031771

Figure 2-1 Weld Overlay Design

NOTES

1. Component surface is to be examined by dye penetrant method and accepted as clean prior to overlay application.
2. In the event that the original component surface does not pass the Note 1 requirements, the final deposited temper bead weld layer is to be examined by dye penetrant method and accepted as clean before proceeding with subsequent layers.
3. Weld overlay wire shall be ERNiCrFe-7 (Alloy 52).
4. The design thickness (0.51 inch) is the minimum thickness beyond the first PT clean layer, and beyond two layers minimum for dilution control. Thickness must be maintained for distance "B". The overlay shall be extended across to blend into the nozzle taper to support of inspection and minimize stress concentration.
5. Apply as many layers as required to achieve the design overlay thickness "t".
6. Design thickness includes no allowance for surface conditioning operations to facilitate UT inspection.
7. Design length is that required for structural reinforcement; greater length may be required for effective UT inspection. This is to be determined in the field.
8. Overlay to be blended gently into nozzle to minimize stress concentration and to accommodate temper bead weld passes. Extra temper bead layers may be applied, approximately 1/8" above blend to facilitate additional layers if necessary.

Job No: TMI-03Q	Plant/Unit: Three Mile Island Unit 1	 STRUCTURAL INTEGRITY ASSOCIATES, INC.	
File No: TMI-03Q-501			
Drawing No: TMI-03Q-01	Title: Standard Weld Overlay Design	Sheet <u>2</u> of <u>2</u>	

031790

Figure 2-2 Weld Overlay Design (cont'd)

3.0 WELD RESIDUAL STRESS ANALYSIS

In addition to providing structural reinforcement to the flawed location to meet ASME Code safety margins, the weld overlay produces beneficial residual stress that supports the mitigation of PWSCC. The weld overlay approach has been used in the BWR industry on hundreds of occasions. There have been no reports of crack extension after application of the weld overlay. Thus, the compressive stress caused by the weld overlay has been effective in mitigating crack growth in BWRs including feedwater nozzles, which are subjected to significant thermal cycling. In addition, the weld residual stress from this calculation is used as a mean stress in the fatigue crack growth assessment.

The weld residual stress was determined for the weld overlay design based on the Section 2.0 calculation. To obtain a bounding assessment of the impact of the weld overlay on the flawed location, the residual stress assessment must consider residual stress that existed prior to application of the overlay. Thus, the weld overlay analysis must consider residual stress that is present due to the as-welded condition and any machining or weld repairs that may have previously occurred.

The original construction of this particular weld involved significant removal of material and welding. The safe end side of the weld was machined significantly after welding. Plant records also indicate that a weld repair was performed on the inside diameter of the pipe and it was likely a near 360° repair. The analytical prediction of weld residual stress is a function of the weld parameters (heat input, bead size, bead placement sequence, etc.), which are not specifically known for the as-welded condition and weld repair. Thus the determination of weld residual stress for this process would contain significant uncertainty in representing the actual stress condition. Due to the significant uncertainty in the initial condition, the goal was to determine the general effect of the weld overlay on a severe as-welded stress distribution (significant tensile stress) that promotes PWSCC.

The approach used to assess the effectiveness of the weld overlay and determination of the weld residual stress was to perform the analytical evaluation of the weld overlay using the residual

stress from a 360° significant ID weld repair. ID weld repairs are known to develop severe residual stress fields and can also provide for flaw initiation sites due to grinding and weld defects. Thus, a fully circumferential 50% of wall ID repair was simulated and the resulting stress field used as the initial stress state for the weld overlay residual stress analysis, illustrated in Figure 3-1. The repair was assumed to be 0.55" deep, with a width of 0.8 inches at the pipe inside surface and tapering to a radius of 0.15 inches at the root of the repair. The width of the Alloy 182 weld butter was assumed to be 0.25 inches thick.

3.1 Weld Parameters

3.1.1 Original ID Weld Repair Weld Parameters

For the ID weld repair, six weld layers were assumed. One bead pass was assumed for the weld root layer. Two bead passes were assumed for the remaining weld repair layers. Typical heat inputs and torch velocities were assumed for the weld repair. A preheat temperature of 200 °F was assumed before the weld root repair, with a maximum interpass temperature of 350 °F.

3.1.2 Weld Overlay Weld Parameters

For the weld overlay, actual weld parameters were used in the analysis [15]. For the weld overlay, the weld torch travel speed was 3 inches/min. The bead width was assumed to be 0.25". The bead thickness for the first layer was assumed to be approximately 0.05" to 0.08". The bead thickness for the subsequent layers was assumed to be 0.08" to 0.1". Therefore, the bead area is modeled as 0.08" by 0.25" wide. These assumptions were only used to calculate the equivalent number of bead passes in the lumped weld passes approach used in the finite element analyses. Similarly, for the weld overlay, three lumped bead passes were used in each of the five layers. The number of equivalent bead passes was estimated from the lump pass areas in the model divided by the area of each bead pass.

The maximum interpass temperature of 350°F was used for the weld overlay. The progression of the overlay welding was from the safe end side to the nozzle side of the weld. A thermal efficiency of 75% was assumed for the welding process in the analyses.

3.2 Finite Element Model

The analyses were performed using ANSYS [7]. The finite element model for the residual stress evaluation is presented in Figure 3-2. Figure 3-2 also presents the material identification in the model and detail in the vicinity of the weld. The axisymmetric model was used for both the thermal and stress passes of the analyses. The weld bead deposit was simulated by the element “birth and death” capabilities in ANSYS. The hot leg was not modeled in detail. This does not affect the residual stress results at or near the weld. A roller boundary condition was applied at the thick nozzle end of the model in the stress pass. Temperature dependent non-linear material properties were used in the analysis as well as an appropriate strain-hardening model.

The analysis consists of a thermal pass to determine the temperature response of the model to each individual lumped pass as it is added in sequence, followed by an elastic-plastic stress pass to calculate the residual stress due to the temperature cycling from the application of each lumped weld pass. Since the residual stress is a function of the welding history, the stress passes for each lumped pass were applied to the residual stress field induced from all previously applied weld passes.

For the thermal analyses, a heat convective boundary conditions with a convection heat transfer coefficient of 5 Btu/hr-ft²-F was conservatively assumed at the surface of the model to simulate the water condition inside the pipe. This is conservative since this is closer to that due to natural convection with air and well below that for water natural convection. Thus, this analysis likely underpredicts the benefit from the weld overlay process.

After the weld overlay was completed, the model was allowed to uniformly cool to a uniform 70 °F, and heated up to a uniform 650 °F in order to obtain the residual stresses at the room and maximum operating/upset temperature.

It is recognized that the subsequent operation of the plant may slightly modify the residual stress field. However, due to the uncertainty of the weld residual stress, the uncertainty in the parameters defining the weld repair and as-welded condition uncertainty in actual material properties, the resulting residual stresses are considered representative of what remains in the weld after experiencing plant operation. It would also be extremely difficult to model the specific effect of all transients and loading conditions on the weld residual stress since even operation differs substantially from that defined in the plant design basis. Weld overlays have been in service at BWR plants for many years, including feedwater nozzles that experience significant thermal loading, and demonstrated their ability to mitigate SCC.

3.3 Residual Stress Results

Figure 3-3 shows the axial and hoop residual stress results after the weld overlay at the operating temperature. As can be seen from this figure, the residual hoop stress is significantly compressive throughout the weld. Even if the pressure hoop stress is added to this, the resulting hoop stress will be significantly compressive and would mitigate PWSCC. Similarly, the axial stress is significantly compressive through much of the cross section at the weld location. Even when the pressure stress is superimposed on this distribution and normal operating thermal stresses, compressive stress remains in much of the cross section. The resulting stress intensity factor distribution supports arrest of the postulated circumferential flaw.

The residual stress results are also used in the fatigue crack growth analysis summarized in the following section.

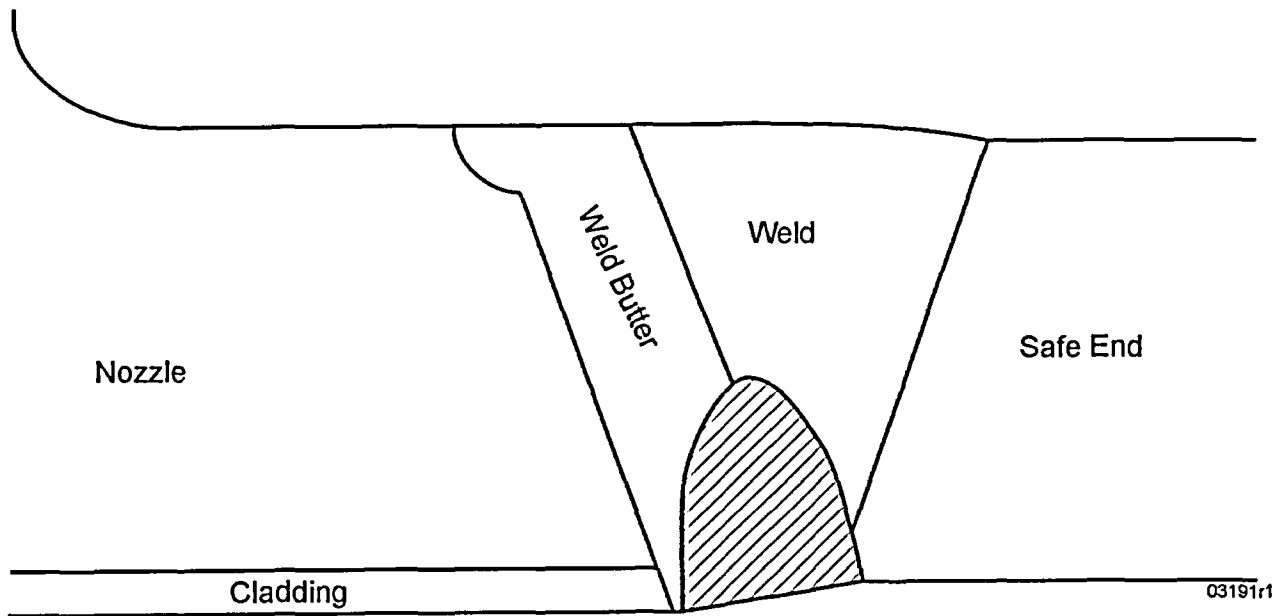
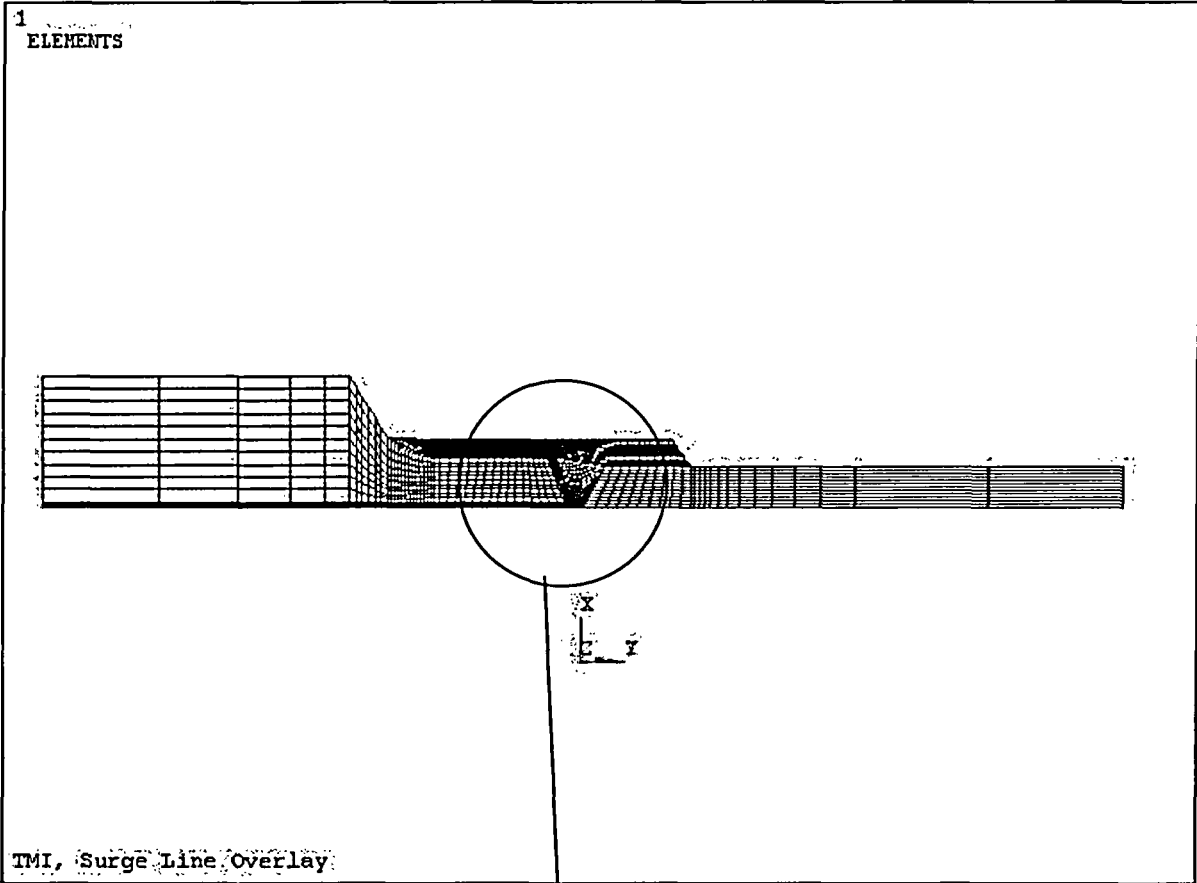
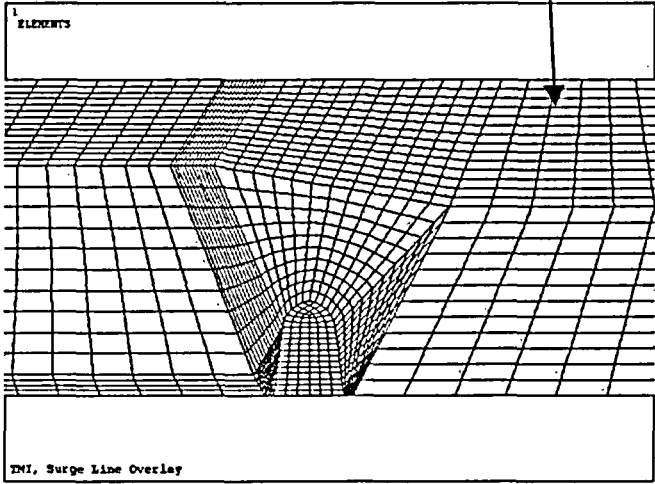


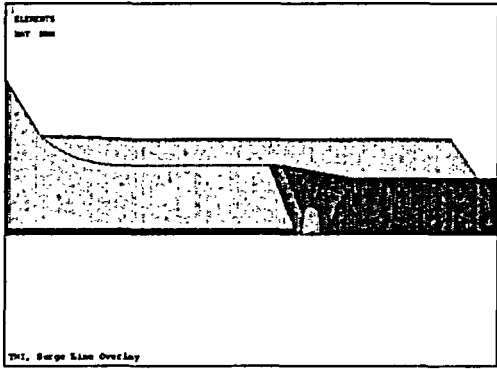
Figure 3-1: Schematic of ID Weld Repair



Overall Finite Element Model

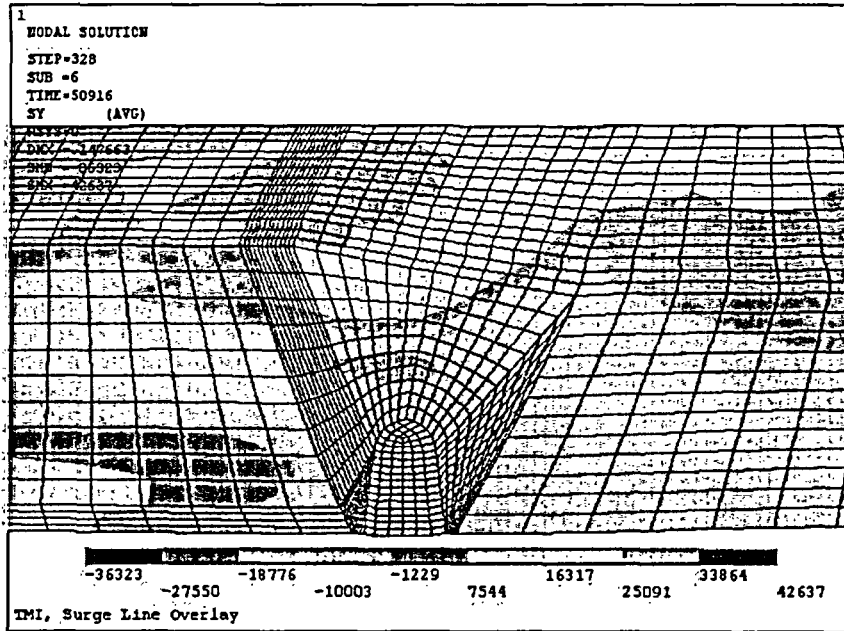


Detail Near Weld

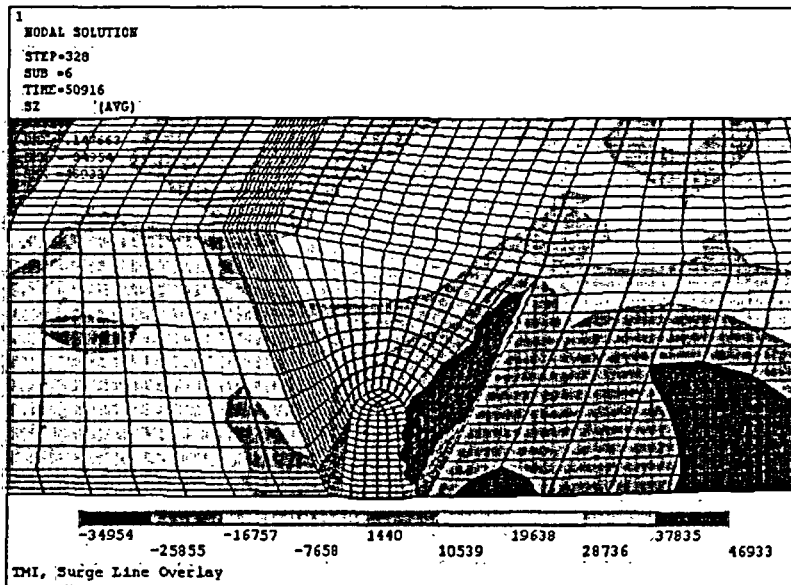


Material Designation

Figure 3-2: Finite Element Model For Weld Residual Stress Analysis



a) Axial Stress



b) Hoop Stress

Figure 3-3: Residual Stress Distribution in Vicinity of Weld Due to Weld Repair and Weld Overlay

4.0 CRACK GROWTH EVALUATION

This section presents the crack growth evaluation due to operation after application of the weld overlay. ASME Code Case N-504-2 requires that the repair consider potential flaw growth due to fatigue and the mechanism believed to have caused the flaw. Recall that the design basis flaw for this weld overlay design is a fully circumferential through-original-pipe-wall flaw, such that this is the allowable flaw size. Only an axial flaw is present at the weld location of interest. There is no evidence that a circumferential crack is present. However, for conservatism, a circumferential flaw will also be assumed for the crack growth evaluation.

To address fatigue and fatigue crack growth effects for the weld overlay the loadings used in this analysis will be those developed for the B&W Owners Group [8] in responding to NRC Bulletin 88-11 [9]. The results of the fatigue crack growth analysis will be used to confirm the weld overlay design that was based on considering PWSCC only (Section 2.0).

The potential for PWSCC after application of the weld overlay will also be addressed. In BWRs, weld overlays have been credited with producing significant compressive stress on the pipe ID and was confirmed for this case by the results presented in Section 3.0.

The fatigue crack growth evaluation will consider stresses due to a number of different loading sources. These load sources were:

- Forces and Moments at the hot leg nozzle location due to hot leg nozzle thermal expansion movements, pressurizer nozzle thermal movements, surge line thermal expansion, surge line stratification, overlay shrinkage and dead weight.
- Surface and through-wall stresses at the weld overlay location that occur due to local stratification at the nozzle, local temperature changes and thermal transients.
- Local residual stresses (including original fabrication repairs) at the overlay and weld location due to weld shrinkage and application of the overlay.
- Pressure.

Based on the results of the analyses listed above, fatigue crack growth analysis was performed for the observed axial flaw with an assumed initial length equal to twice the depth (essentially the full width of the weld at mid-wall). A postulated circumferential flaw of the pipe thickness with an aspect ratio of 10:1 (l/a) circumferential on the inside surface was also evaluated. The number of operating cycles to grow each of the flaws to the ASME Code Section XI allowable flaw size (corresponding to the thickness of the original safe end) were determined.

It is important to distinguish the design basis for the overlay versus the crack growth assessment. The design basis flaw for the overlay design is a 360° through-wall flaw. The crack growth assessment is performed on the actual flaw found and to be conservative, a circumferential flaw is also postulated.

4.1 PWSCC

This section describes the assessment for PWSCC of the overlaid flaw. For PWSCC to occur, tensile stress is necessary to drive the flaw through-wall as well as lengthwise. The stress intensity factor (K_I) is the parameter that determines if crack growth can occur.

4.1.1 Axial Flaw Crack Growth

The axial flaw driving force is the hoop stress due to those sustained stresses that are present during normal operation. For the axial flaw, hoop stress due to residual stress and pressure stress are the only stresses of concern. As shown in Section 3.0, the residual stress at the flawed cross section is significantly compressive (≥ 20 ksi compression) through much of the pipe wall. Even when the hoop stress due to pressure ($\cong 10$ ksi) is superimposed on the residual stress, the stress remains compressive. Even if some relaxation were to occur due to pressurization and other loadings, it is expected that significant compressive stress would remain. This results in a negative stress intensity factor throughout the entire wall even when the K_I from pressure is

added. Since PWSCC does not occur under compressive stress (when stress intensity factor is negative), the overlay mitigates PWSCC of the observed axial flaw.

Thus, if only PWSCC were being considered, no growth of the observed axial flaw would be expected.

4.1.2 Circumferential Flaw Growth

The circumferential flaw driving force is the axial stress due to the sustained stresses that include pressure, residual stress and other thermally induced sustained stresses. Recall that no circumferential flaw has been found. This analysis is performed to evaluate the potential for growth from a postulated circumferential flaw. The axial residual stress is slightly tensile very near the surface, but then becomes significantly compressive a short distance into the pipe wall. Even after adding the other sustained stresses, PWSCC of the postulated circumferential flaw would not be expected to penetrate the original pipe thickness.

4.1.3 Alloy 52 PWSCC

The weld overlay material is Alloy 52 (UNS N06052, Alloy 52, ASME Code Case 2142) applied over the [REDACTED] weld and [REDACTED] safe end. Generic Letter 88-01, which addresses stainless steel weld overlays, discusses a dilution layer when welding over austenitic stainless steel, which requires that the first layer not be considered as IGSCC resistant if it does not have a ferrite level of 7.5% (or 7.5 FN). This situation does not exist in nickel base alloys (such as Alloy 52) since there is no ferrite and the PWSCC resistance comes generally from the high level of chromium in the alloy. Consequently, the initial layer can be retained as PWSCC resistant provided the chromium level is sufficient. It is believed that a chromium level of approximately 25% is required to provide outstanding PWSCC resistance for nickel-based materials in the PWR environment.

When diluted with carbon steel (containing essentially no chromium), it is anticipated that the chromium level of the diluted first layer produced by an Alloy 52 weld overlay would be of the

order of 15-20%, dependent upon the "bite" taken from the base material (which in this case would be carbon steel) to form the weld puddle. Consequently, the diluted "first layer", or 0.075-inch (nominal), would likely not be resistant to PWSCC and therefore should not be counted as a PWSCC resistant layer. By the completion of the second layer, the chromium level of the deposit should approach 25% chromium, thereby producing a deposit, which is resistant to PWSCC. In this overlay design, both the first and second layers are not counted as PWSCC resistant as an additional design conservatism.

No crack propagation is anticipated into the carbon steel nozzle and stainless steel safe end. These materials are extremely resistant to stress corrosion cracking in the PWR environment. Cyclic loading requires high load amplitudes to produce environmentally assisted cracking in carbon steels in the BWR environment.

In summary, welding with the chromium rich Alloy 52 generally provides a PWSCC resistant material after two layers even when diluted with carbon steel.

4.1.4. PWSCC Conclusion

Results of this assessment show that PWSCC growth of the observed axial flaw will not occur due to the significant compressive stress induced by the weld overlay. For the postulated circumferential flaw PWSCC will not penetrate the original pipe wall due to the significant compressive stress induced by the weld overlay in the center of the pipe. Thus, PWSCC growth is not considered further. Even if PWSCC were not fully mitigated, PWSCC beyond the original pipe wall (including the two layers for dilution) would be unlikely due to the highly resistant Alloy 52 material.

This conclusion is consistent with similar results for BWR weld overlays. In BWRs, weld overlays were credited with producing beneficial compressive stresses that mitigated IGSCC. Field experience for hundreds of overlays has demonstrated no evidence of subsequent crack growth, consistent with the conclusion that weld overlay mitigates IGSCC in BWR plants. Note that weld overlays have been applied to BWR feedwater nozzles that are subjected to significant

thermal cycling. Performance at these locations has been similar to other BWR weld overlay locations.

4.2 Fatigue Crack Growth

This section describes the fatigue crack growth analysis to demonstrate acceptability of the weld overlay design shown in Section 2.0. ASME Code Case N-504-2 requires that fatigue crack growth be considered. The evaluation considers both the actual axial flaw and a postulated circumferential flaw, initiating at a size that may have been missed by inservice inspection. The objective of the calculation is to determine the number of heatup/cool-down cycles required to grow the flaws to a depth equal to the original pipe thickness, or to determine the flaw size based on the number of plant design transients. These results can be used to confirm the weld overlay design from Section 2.

4.2.1 Fatigue Crack Growth Technical Approach and Methodology

The crack growth analysis is based on the concepts of linear elastic fracture mechanics (LEFM). All significant loadings on the surge line and the region at the nozzle-to-safe-end weld are considered, including:

- Dead weight nozzle moment and axial force loadings.
- Nozzle moment and axial force loading due to an assumed 0.25" axial shrinkage due to weld overlay application.
- Surge line thermal expansion moments and axial forces (for varying temperature conditions).
- Hot leg and pressurizer nozzle movement moments and forces (for varying temperature conditions).
- Moments and axial forces generated due to thermal stratification in the lower horizontal surge line and the horizontal segment of piping adjacent to the hot leg nozzle (for varying stratification conditions).
- Weld residual stresses (after application of the weld overlay).
- Temperature dependent stresses at the weld due to elevated temperature conditions.
- Local stratification stresses at the weld location.
- Pressure through-wall stress distribution.
- Through-wall thermal stress distributions for thermal transients.

Stresses were determined for all of the above listed loads. Through-wall stress distributions were obtained for use in the fatigue crack growth calculations.

The pipe and weld overlay were modeled per the appropriate dimensions with the overlay design shown in Section 2.0. For purposes of crack growth analysis, the initial inspection results showed that an axial crack existed with a depth of 0.51", which included uncertainty. In addition, although there is no indication that a circumferential flaw exists, a postulated circumferential flaw was analyzed with an initial depth of 0.11" (█
█). Thus, the following flaws were assumed for this analysis:

- Axial Flaw: 0.51" depth by 1.1" length, representative of the weld width at the mid-wall position at the observed crack depth. The aspect ratio will be held constant during crack growth, such that at near 1" depth, the length would be approximately 2".
- Circumferential Flaw: 0.11" depth with a constant aspect ratio (flaw length to flaw depth) of 10 to 1.

The Framatome (FANP) Functional Specification for the surge line [8] forms the basis for all loading conditions considered in the crack growth analysis. Information was obtained that defined the specific loadings used by Framatome for the B&W Owner's Group surge line evaluations performed in response to Bulletin 88-11 [9]. This information was evaluated to determine the following specific information for all significant design transient stress extremes (peaks and valleys) at the hot leg nozzle-to-surge line weld:

- Pressurizer pressure and temperature
- Hot leg temperature.
- Temperature in each of the surge line segments.
- Stratification in the surge line lower and hot leg piping segments.
- Maximum rate of temperature change in the hot leg nozzle region leading up to each stress peak or valley.
- Level of stratification in the hot leg nozzle for each stress peak or valley. (The level in the lower surge line was assumed to be at the center of the pipe producing maximum bending moments at the nozzle.)
- Maximum flow rate in the piping system associated with each stress peak and valley.
- Specific definition of cycling and number of cycles for each design event.

Note that a few of the minor plant design transients were determined to not be significant and were thus not specifically evaluated, consistent with evaluations conducted by the B&W Owner's Group to support the NRC Bulletin 88-11 response.

Piping stress analysis was performed for the surge line to develop moments and forces for "unit" loading conditions. These unit conditions were adjusted based on the actual conditions for each stress cycle. Forces and bending moments are modified to the appropriate conditions for each evaluated state for the transients by multiplying the forces and moments by the ratio of the state temperature in the segment (minus 70°F) to the temperature change used in the piping analysis that was performed to develop the "unit" loads.

The global moments generated by a stratified piping section depend both on the local heat transfer coefficients, vertical distribution of temperature and level of the hot/cold interface. For this analysis, factors were developed as a function of nominal flow velocity in the pipe and stratification interface height to adjust the unit local moments from the piping analysis. The water was conservatively held at the hot top temperature above the interface and at the cold bottom temperature below the interface. These multipliers were used only for the short piping section adjacent to the hot leg nozzle, since similar information was not available at the time of the analysis to adjust the moments in the lower piping section. For the lower piping, the maximum effects of stratification were included for the condition of hot water in the top half of the pipe and cold water in the lower half. In addition, a multiplier was applied to adjust the moments at the nozzle to account for the top-to-bottom temperature difference compared to that used in the "unit" load piping analysis for stratified conditions.

Axial forces from the piping were assumed to develop uniform stress distributions (membrane stress) at the weld. The stresses due to bending moments were assumed linearly distributed across the pipe total cross section for each of the orthogonal moments at the cross section.

Local axial and hoop stratification through-wall stress distributions were developed around the circumference for several different stratification levels based on bounding heat transfer coefficients using a detailed three-dimensional finite element model.

Axisymmetric hoop and axial through-wall stresses distributions were used for several types of loads:

- Weld overlay residual stresses, assumed to be constant.
- Bimetallic stresses at the weld due to differential thermal expansion of the materials at the weld (function of temperature at the top of the nozzle region).
- Pressure stresses (adjusted for the actual pressures for each state).
- Temperature gradients due to inside temperature change of the fluid in the top of the nozzle region (that was shown to experienced the most temperature cycling).

In consideration of thermally induced through-wall stresses, the Framatome-supplied loadings reflected in Reference 8 had

[REDACTED]. The analysis was conducted to determine the through-wall gradient stresses for long ramp transients (where through-wall stress distributions are quasi-steady) and for step change transients, both as a function of flow rate in the nozzle. For some relatively short transients, the ramp-change stress results were over-conservative, since the quasi-steady stress distribution could never be developed. In these cases, the stresses were bounded by applying the step change transient stresses based on the temperature change in the top of the nozzle occurring since the previous stress peak or valley. This is conservative since the change in temperature since the last stress peak and valley likely occurred not as a step, but as a type of ramp transient that would produce lower stresses than the step change assumed.

The crack models for both axial and circumferential cracks were taken from the EPRI Fracture Mechanics Handbook [10]:

- Circumferential Flaw: Model for semi-elliptical part-through-wall flaw (page 3.1-23 of [10]). Since the model had a mean radius to thickness ratio validity range of $5 < R/t < 20$, and the nozzle with weld overlay creates a ratio that is slightly less than this, the R/t parameter in the model was assumed to be $R/t = 5$.
- Axial Flaw: Model for finite length axial part-through-wall flaw (page 8.1-51 of [10]). The formulation specifically considered the dual G_0 coefficients that considered the actual values for the crack parameters as a function of $a/c > 0.2$ and $(a/t)/(a/c)^m > 2$.

4.2.2 Crack Growth Rate

The crack growth law for Alloy 600 was used for the weld material [11]. This has been converted to a crack growth law with environmental effects as follows:

$$da/dN = (da/dN)_{air} + A \times T_r^{1-m} \times (da/dN)_{air}^m \quad (4-1)$$

where: da/dN = crack growth rate, m/cycle

$$A = 4.4 \times 10^{-7}$$

T_r = rise time, seconds

$$m = 0.33$$

$$(da/dN)_{air} = C_{A600} (1-0.82R)^{-2.2} (\Delta K)^{4.1}$$

$$C_{A600} = 4.835 \times 10^{-14} + 1.622 \times 10^{-16} \times T - 1.49 \times 10^{-18} \times T^2 + 4.355 \times 10^{-21} \times T^3$$

T = temperature in top of pipe, °C

R = R-ratio (K_{min}/K_{max})

ΔK = range of stress intensity factor, $Mpa\sqrt{m}$

As recommended in [11], a maximum multiplier of 10 was applied to this crack growth rate to account for the differences between base material and weld material.

Although most of the rise time testing in [11] was reported as being conducted at times on the order of one second, the rise time was reported for weld metals was up to 5000 seconds. For this analysis, rise times were calculated by dividing the change in temperatures from one load state to the next by the rate of temperature change. In a few cases, the rate of temperature change provided was extremely low and the temperature changes were very small, producing unrealistically high rise times. In these few cases, a maximum rise time of 5000 seconds was assumed.

To test the effects of the Alloy 600 weld crack growth law above against previous work, the analysis also considered the austenitic steel crack growth law from Section XI of the ASME Code [1]. As recommended in the Code basis document, a factor of two was applied to account for PWR environment [12]. (This confirmed that the Alloy 600 crack growth law was much more conservative).

In performing the analysis, the crack growth was determined based on each rising stress intensity factor (K_I) period and each decreasing K_I interval separately, assigning a $0.5 \times da/dN$ to each half cycle. It was assumed that the rise time for the increasing K_I period was also applicable to the next decreasing K_I period. In certain cases, the computed stress intensity factors contained an intermediate state between a valley and a peak that could be deleted, such that the larger encompassing ΔK range was considered. In this case, the assumed rise time was taken as the maximum of the two rise times before and after the discarded intermediate point since this would maximize the crack growth rate associated with the ΔK range.

4.3 Fatigue Crack Growth Analysis Procedure

The analysis procedure included the following:

- Obtain from an input file; transient conditions, unit moments, through-wall stress distributions, etc.
- Determine a weld location (from an input range of locations) around the pipe circumference for analysis.
- Compute the resulting crack growth for each heatup/cooldown (HU/CD) cycle.
 - For each of the load steps for each design transient, compute the moment loadings at the nozzle and the resulting stress coefficients for all contributors to stress. Sum the stress coefficients for all loadings.
 - Compute the stress intensity factor for each load step.
 - Compute the rise time for each peak stress intensity factor.
 - Eliminate any intermediate peaks/valleys.
 - Compute the crack growth for the series of peaks and valleys, updating the crack size after each design transient. Since the crack growth analysis is computed on a per heatup/cooldown cycle, a fraction of the computed crack growth for each design transient is used that is proportional to the total cycles of each transient divided by the total number of heatup/cooldowns. This approach spreads the effects of transients uniformly over time.
- Repeat the above steps over all [REDACTED] design heatup and cooldown cycles or until the crack size reaches the assumed allowable size equal to the safe-end thickness of [REDACTED].

As mentioned earlier, calculations were performed using the crack growth rate from [11] and also using the austenitic steel crack growth law for ASME Code Section XI [1]. The analysis was also performed for the actual axial crack and the postulated circumferential crack.

4.4 Results of Fatigue Crack Growth Analysis

The results of this analysis are summarized in Table 4-1. Figures 4-1 and 4-2 show the crack depth as a function of the assumed crack location (degrees from pipe top-dead-center) around the circumference of the nozzle-to-safe end weld. The number of acceptable HU/CD cycles is 217 based on the actual observed axial flaw. For the postulated circumferential flaw, the allowable number of HU/CD cycles is 70. The crack growth for the axial crack is quite uniform regardless of the angular location of the crack. The actual flaw is located approximately 25° from top-dead-center. There is significantly more variation around the circumference for the amount of crack growth for the postulated circumferential crack. The crack growth at the bottom of the pipe is less than at other circumferential locations due to a favorable combination of pipe bending and local stratification stresses. The low crack growth location is in the region below the stratified interface. As can be seen in Figure 4-2, a postulated circumferential flaw reaches the maximum depth at around 100° from top-dead-center.

To assure that there was not a combination of conservatively high thermal stresses that combined with stratification stresses that might be retarding crack growth, a second set of runs was completed with the through-wall stresses due to thermal transients suppressed. These results are also shown in Table 4-1.

Table 4-1 (and Figures 4-1 and 4-2) also show that the primary contributor to crack growth is the thermal transients and not stratification cycling. With the through-wall thermal stresses suppressed, the crack growth at all locations is much less than when the thermal stresses are included. The presence of the weld overlay further reduces the stresses due to piping thermal expansion, nozzle anchor movements and thermal stratification, which are already quite low without the overlay, such that the stratification-induced moment cycling is not the significant contributor.

It is also of interest to observe the source of the crack growth. In Figure 4-3, the relative contribution of all transients (e.g., T1A1 is a [REDACTED] from the surge line functional specification [8]) is shown for the most limiting assumed circumferential

crack as reported in Table 4-1. This shows that over 65 percent of the crack growth is attributed to the [REDACTED] transients. The amount of crack growth is not due to the severity of the transients, but is due to the fact that [REDACTED] are specified to occur [REDACTED] times for each heatup/cooldown event. For the plant design transients with [REDACTED] heatup/cooldown cycles in [REDACTED] years, this corresponds to bringing the plant to [REDACTED] power and then increasing to [REDACTED] [REDACTED] times per day, which is not representative of the actual plant operation. Thus, if actual plant cycling behavior were considered, much lower crack growth would be calculated such that this analysis is considered very conservative relative to actual plant operating conditions. In addition, the number of actual plant HU/CD cycles is much less than assumed in this analysis.

Another observation that may help with respect to inspection frequency is gained from Figure 4-4. For the postulated circumferential crack, the crack depth versus number of operating cycles is shown. Since the major contributor to the stress intensity factor cycling is through-wall thermal stresses (with ranges that diminish through the wall), the crack-growth rate is relatively constant with number of cycles. This is of benefit for inspection-based fatigue management in that there is no expected sudden increase in crack size as the crack approaches the allowable flaw size at the safe-end/weld overlay interface ([REDACTED]) in this analysis.

The results of this analysis indicate that even with the conservative assumptions made in the analysis, using the weld overlay design is acceptable for 217 heatup/cooldown cycles based on the actual observed axial flaw. If the postulated circumferential flaw is considered, the number of allowable HU/CD cycles is 70. Based on these results, no modification to the weld overlay design in determined in Section 2 is necessary to accommodate fatigue crack growth.

4.5 Final Weld Overlay Design

Based on the discussion above, Figure 2-1 and 2-3 is the final weld overlay design. This design meets the ASME Code Section XI safety margins and stress limits. Based on the results of the fatigue crack growth analysis, no change is needed to the weld overlay design to compensate for fatigue crack growth.

Table 4-1: Crack Growth Results

Flaw Case Description and Crack Growth Curve Used	Flaw Depth and Length	
	Axial Flaw	Circumferential Flaw
Initial Depth and Length (Aspect Ratio a/c)	0.51" x 1.1" (a/c = 0.927)	0.11" x 1.1" (a/c = 0.2)
Final Depth (2 x 1998 ASME Section XI Curve)	0.54" after [REDACTED] HU/CD cycles	0.26" after [REDACTED] HU/CD cycles
Final Depth (10 x Alloy 600 Base Metal Curve)	[REDACTED] after 217 HU/CD cycles	[REDACTED] after 70 HU/CD cycles
Final Depth (2 x 1998 ASME Section XI Curve) TW Thermal Stresses Suppressed	0.5101" after [REDACTED] HU/CD cycles	0.1104" after [REDACTED] HU/CD cycles
Final Depth (10 x Alloy 600 Base Metal Curve) TW Thermal Stresses Suppressed	0.54" after [REDACTED] HU/CD cycles	0.62" after [REDACTED] HU/CD cycles



Figure 4-1: Final Crack Size for Axial Crack in Weld



Figure 4-2: Final Crack Size for Postulated Circumferential Crack in Weld

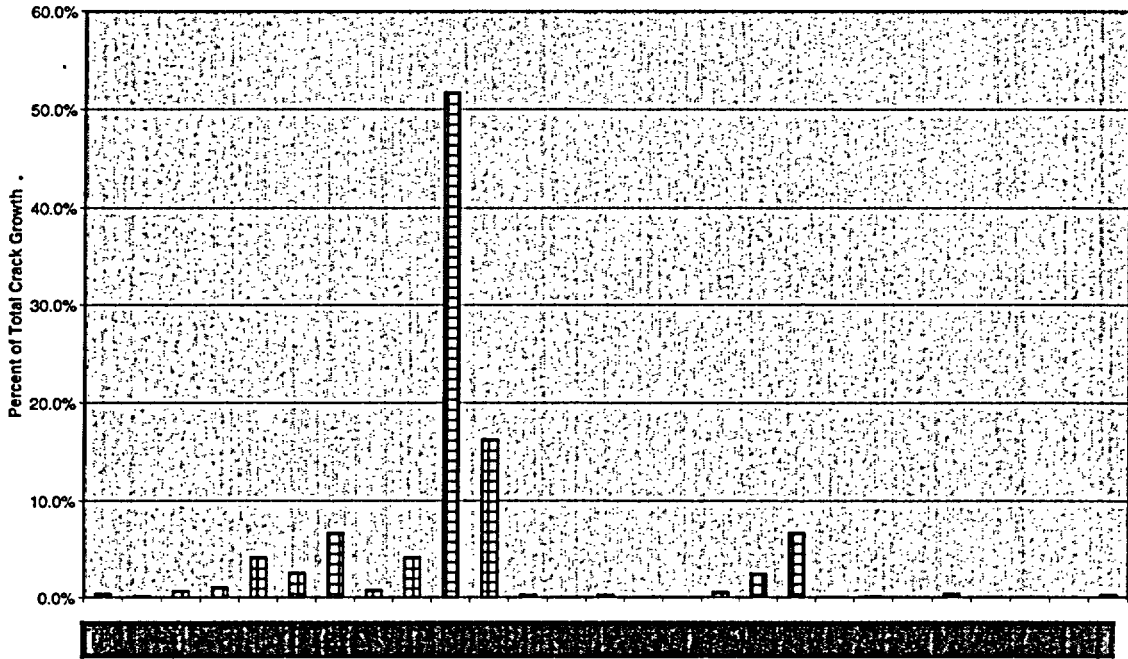


Figure 4-3: Contribution of Various Transients to Crack Growth Postulated Circumferential Crack for Alloy 600 Crack Growth Rate

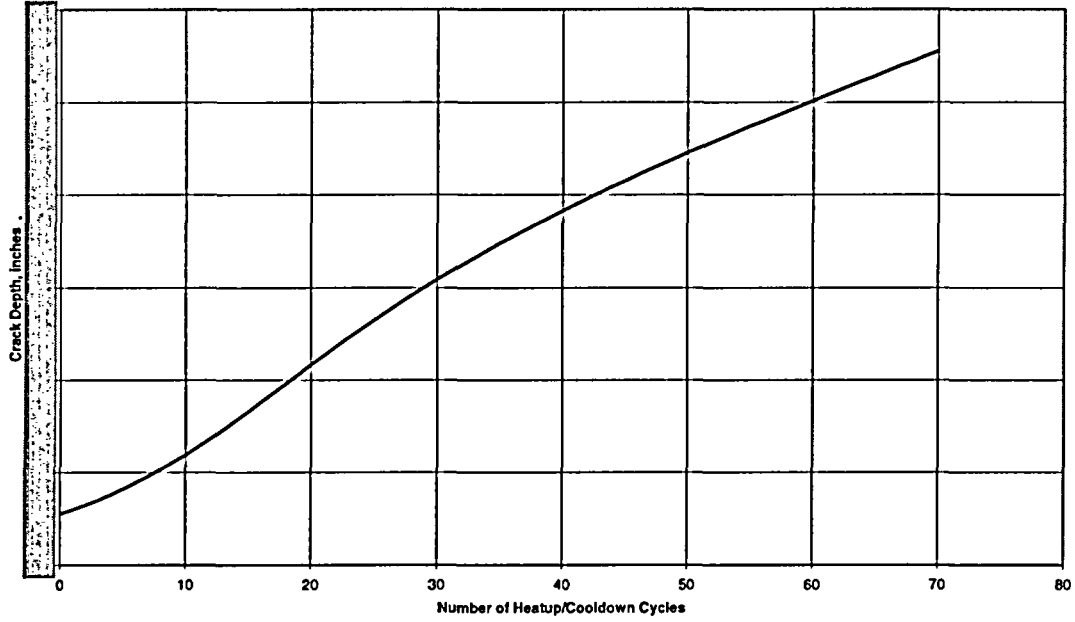


Figure 4-4: Crack Growth for Postulated Circumferential Crack – Alloy 600 Crack Growth Law

5.0 STRESS REPORT RECONCILIATION

This section presents the discussion of the impact of the weld overlay application on the Design Stress Report for the nozzle/piping. The original stress report was performed using the [REDACTED] Code. The following assessment of the impact of the weld overlay is presented to illustrate that the presence of the overlay does not invalidate the current nozzle design basis stress report. Of specific interest are the changes in stress and the impact on fatigue usage.

With respect to primary stresses, the addition of the overlay material could potentially add to the existing deadweight and seismic inertia stresses. The nozzle moments due to dead weight were shown to be very small. The added weight due to the weld overlay is considered insignificant compared to the weight of the piping and the safe end. Hence, the current stress analysis of the piping and nozzle will not be significantly impacted by the weight of the weld overlay material. In addition, the stiffness of the piping will not be significantly affected by the relatively short overlay. Therefore, the dynamic characteristics of the piping will not be significantly affected and seismic moments will remain unchanged.

In order to assess the general impact of the weld overlay on the nozzle, finite element analyses were performed for the nozzle/safe end region using models both with and without the overlay in place. The analyses were performed using both pressure and a representative thermal transient. It is recognized that there are many variations for thermal cycling conditions, but this comparison serves to evaluate the general impact of the overlay. Thus, two loading conditions were applied to the axisymmetric finite element models to assess the difference between the nozzle and safe end with the overlay and the original condition. The first case was that for internal pressure and the second case was a thermal transient [REDACTED], representative of the worst stratification transient occurring during heatup [8]. Thus, this thermal condition represents a worst case transient in terms of temperature change and rate of change.

Comparison of the stresses in the nozzle area, toward the RCS piping from the weld overlay, showed that the resulting total stresses for both the pressure and thermal case were essentially

identical in both models. This demonstrated that the weld overlay does not have a significant impact on the stress and fatigue usage results of the design basis stress report for the nozzle area. Thus, the existing design basis stress report for the nozzle remains valid with the weld overlay applied.

In the general area of the weld overlay, comparison of the stress results with and without the overlay indicate that, except for the end of the overlay-to-nozzle outside diameter location, the total stress is not impacted significantly. The added weld overlay material significantly increases the thickness of the wall, thus reducing the pressures stress. Similar reduction would occur for bending loads from the attached piping. The overlay to nozzle taper is blended to reduce any stress intensification at this region.

At the location of the as-welded dissimilar metal weld, most of the thermal stresses occur due to the bimetallic thermal expansion effect so there was not a significant change in these stresses due to the thermal transient. The pressure stresses (and also the piping bending stresses) at this location are reduced due to the increased thickness. At this location, the previously described crack growth analysis is used to qualify the fatigue status, so the comparison of the usage before and after the weld overlay is not required.

The most significant change of the stresses was observed in the safe end, at the end of the weld overlay where it is terminated at the outside surface of the stainless steel safe end. The new weld overlay configuration involves a thickness and geometric transition since it is located at the end of the weld overlay taper which has at most a 45° angle of intersection with the outside surface of the pipe that is blended onto the safe end to avoid stress concentration. This transition is more severe than the transition in the original as-welded condition where a transition from a wall thickness of 1.125 to 1.375 occurred. From the finite element stress analysis, the combination of stresses due to the thermal transient and the bimetallic effects at the outside surface discontinuity for the weld overlay is about 2.5 times more than that observed for the unoverlaid configuration. The pressure (and bending moment) stresses were observed to be approximately the same. Based on this comparison, it is recognized that there may be a change to the stress and

fatigue results for the location where the overlay meets the pipe on the outside surface. This effect is not expected to be large, and can be evaluated to end of life in a separate analysis. The results of this comparison indicate that the previously limiting fatigue usage location stress and fatigue usage factor results should remain valid.

6.0 CONCLUSIONS

This report has presented the weld overlay design for the TMI Unit 1 hot leg nozzle-to-surge line weld. The overlay design was based on the requirements of ASME Case N-504-2. The weld overlay minimum thickness and minimum length was determined in accordance with the Code Case. Per Code Case N-504-2, the weld overlay thickness was calculated using ASME Code Section XI IWB-3640, which provides the criteria for flawed piping, based on stress and limit load methodology. In addition, the ASME Code requirement that no flaw can exceed 75% of the total wall was used to determine the overlay thickness. Based on the results of the calculation, the 75% of wall criteria governed resulting in a required structural weld overlay thickness of 0.51”.

The weld overlay was designed using a design basis flaw that was through-original-safe-end-wall and fully circumferential. It is important to note that the actual observed flaw was a short axial flaw that was only about 50% through-wall in depth. There was no indication that a circumferential flaw was present at this location. Thus, the weld overlay design is considered conservative for the actual observed axial flaw.

Code Case N-504-2 requires that the weld overlay design consider fatigue crack growth and the mechanism thought to be the cause of the cracking. The mechanism responsible for the cracking is believed to be PWSCC since it is consistent with previously observed PWSCC and the inspection characteristics of the flaw are consistent with PWSCC and not fatigue cracking.

The weld overlay design is applicable to PWSCC since even if a flaw were to grow through-wall, the Alloy 52 material is highly resistant to PWSCC. Two initial layers of Alloy 52 were applied prior to the start of the structural portion of the weld overlay in consideration of the diluted material. A weld residual stress analysis was performed to demonstrate the effect of the weld overlay on the observed flaw. The weld overlay analysis used the actual weld parameters used to apply the overlay. In addition, a severe ID weld repair was applied prior to the weld overlay to verify the effectiveness of the weld overlay in overcoming a previously existing

residual stress field. Results of the weld residual stress analysis showed that the weld overlay would be effective in mitigating PWSCC.

Since this location is subjected to significant thermal cycling, a fatigue crack growth analysis was also performed. The primary reason for performing this calculation was to verify that the weld overlay design would also be sufficient to assure structural integrity if some fatigue crack growth were to occur. A detailed analysis was performed using the plant surge line functional specification transients. Stresses included those due to stratification (local to the nozzle and in other parts of the surge line), thermal expansion, pressure, seismic, weld residual stress and weld shrinkage (due to overlay). For this analysis, fatigue crack growth was predicted for the actual axial flaw and for a postulated 10% of wall circumferential flaw.

Results of the fatigue crack growth analysis demonstrated that the axial flaw grows to the allowable depth of 0.25 (depth of the original pipe wall) in 217 heatup/cooldown cycles. For the postulated circumferential flaw, the allowable number of heatup/cooldown cycles is 70. Since 1990, TMI Unit 1 has had an average of less than one heatup/cooldown cycle per year. Assuming one heatup/cooldown per calendar year results in a design life of 70 years based on the postulated circumferential flaw results. This exceeds the remaining original licensed operating term plus 20 years of license renewal.

An evaluation of the impact of the weld overlay on stress and fatigue limits for the nozzle showed that considerable fatigue life remains, but further evaluation is needed to exactly quantify the usage factor. It is considered likely that the fatigue usage factor at the end of the overlay where it terminates on the outside surface of the stainless steel safe end, will be bounded by the limiting fatigue usage factor in the current design stress report that was based on conservative assumptions.

7.0 REFERENCES

1. ASME Boiler and Pressure Vessel Code, Section XI, 1995 Edition with Addenda through 1996.
2. ASME Boiler and Pressure Vessel Code, Section XI, Code Case-N-504-2.
3. United States Nuclear Regulatory Commission, NUREG-0313, Revision 2, "Technical Report on Material Selection and Processing Guidelines for BWR Coolant Pressure Boundary Piping," January 1988.
4. 
5. ASME Boiler and Pressure Vessel Code, Section III, 1989 Edition.
6. Structural Integrity Associates, pc-CRACK™ for Windows, Version 3.1, February 1999.
7. ANSYS/Mechanical, Release 6.1, ANSYS, Inc., UP20020321, March 2002.
8. 
9. NRC Bulletin 88-11, "Pressurizer Surge Line Thermal Stratification," U.S. Nuclear Regulatory Commission, December 20, 1988
10. NP-6301-D, "Ductile Fracture Handbook," Electric Power Research Institute, June 1989
11. NUREG/CR-6721, "Effects of Alloy Chemistry, Cold Work, and Water Chemistry on Corrosion Fatigue and Stress Corrosion Cracking of Nickel Alloys and Welds," U.S. Nuclear Regulatory Commission (Argonne National Laboratory), April 2001
12. ASME Section XI Task Group for Piping Flaw Evaluations, ASME Code, "Evaluation of Flaws in Austenitic Steel Piping," *Journal of Pressure Vessel Technology*, Vol. 108, August 1986, pp. 352-366.
13. USNRC, Generic Letter 88-01, "NRC Position on IGSCC in BWR Austenitic Stainless Steel Piping, January 1988, with Supplement 1," February 1992.
14. 
15. Welding Procedure Specification #WPS-01-08-T-801, Welding Services, Inc., November 13, 2003.